Aerosol and Air Quality Research, 18: 1168–1182, 2018

ISSN: 1680-8584 print / 2071-1409 online
doi: 10.4209/aaqr.2017.12.0574

Meteorological Influences on Tropospheric Ozone over Suburban Washington, DC

Mayra I. Oyola[1*], Anna Schneider[2], James Campbell[3], Everette Joseph[4]

[1] *American Society for Engineering Education /Naval Research Laboratory, Monterey, CA 93940, USA*
[2] *NOAA National Weather Service, San Francisco Bay Area, CA 93943-5005, USA*
[3] *Naval Research Laboratory, Monterey, CA 93943, USA*
[4] *University at Albany, State University of New York, Albany, NY 12222, USA*

ABSTRACT

During the NASA DISCOVER-AQ (Deriving Information on Surface conditions from Column and Vertically Resolved Observations Relevant to Air Quality) campaign conducted in July 2011 across metropolitan Washington, DC, 25 daytime ozonesondes were launched from the Howard University Beltsville Campus (HUBC), representing the highest temporal density of measurements ever taken over the region. Time-height depiction of ozone concentration reveals considerable variability near the surface and in the mid/upper troposphere. Meteorological influences are assessed using the synoptic and mesoscale information, which revealed that periodic stratospheric intrusion of ozone-rich air was the main mechanism for elevated levels in the upper troposphere. It is also shown that high concentrations of ozone prevalent in the free troposphere were due to a combination of advection and aged air masses, which accounted for over 40% of the total budget. Poor air quality episodes with high surface concentration were due local emissions of precursors and associated synoptic-scale conditions. Breaks in the elevated ozone concentrations in the boundary layer and free troposphere occurred from frontal passages and accompanying storms. In the most unusual case (26 July, 2011), the combined effect of storms followed by two frontal passages and high pressure positioned west of the region led to decrease column ozone as much as 70%. The unusually deep extent of the reduction appears to be related to the temporary cutoff of air advected from fire locations and polluted regions, which dominated the upper troposphere throughout the period.

Keywords: Tropospheric ozone; Stratospheric injections; Laminar analysis; Meteorological influence on ozone; NASA DISCOVER-AQ; Beltsville; MD.

INTRODUCTION

Elevated levels of tropospheric ozone (O_3) can be very hazardous to human health, therefore its surface concentrations are continuously monitored in order to issue air quality alerts to the general public (Bell *et al.*, 2004). Tropospheric O_3 is primarily formed via photochemical reactions entailing nitrogen oxides (NO), carbon monoxide (CO), and volatile organic compounds (VOCs). Conversely, it can also be produced via interaction of regional pollution with convection and photochemical reactions resulting from lightning-generated nitric oxide (NO) (Thompson *et al.*, 2007a, b; Thompson *et al.*, 2013). Having an understanding of the prevalent weather conditions before, during and after poor air quality events is important as weather patterns influence production and transport of O_3 and its precursors. For instance, the direction and strength of the wind combined with the amount of incoming solar radiation and cloud cover can affect O_3 production rates and transport through advection. Under favorable conditions with strong sunlight and high temperatures, emissions of VOCs and the combination of NO and nitrogen dioxide (NO_2) produce O_3, with the highest concentrations tending to occur at distances a few tens of miles downwind of urban centers.

Nevertheless, this understanding cannot be limited to just monitoring surface conditions, as downward transport of air from the entire atmospheric column can contribute to relative O_3 maxima near the surface and above (Neu *et al.*, 1994; Zhang and Rao, 1999; Aneja *et al.*, 2000; Yorks *et al.*, 2009; Morris *et al.*, 2010; Tong *et al.*, 2011). For example, stratospheric intrusions of O_3, ignited through tropopause folding events, are one of the responsible mechanism for high O_3 variability throughout the entire column (Yorks *et al.*, 2009; Hu *et al.*, 2011; Thompson *et al.*, 2013). Therefore, vertical characterization of O_3 profiles from surface to the lower stratosphere, combined with knowledge of the prevalent atmospheric conditions is of utmost importance.

[*]Corresponding author.
E-mail address: mayra.oyola.ctr@nrlmry.navy.mil

We describe the synoptic and mesoscale meteorological drivers influencing O_3 profile variability in the Washington, DC area during the NASA Deriving Information on Surface conditions from Column and Vertically Resolved Observations Relevant to Air Quality (DISCOVER-AQ) campaign conducted in July 2011 across metropolitan Washington, DC. The observations described were obtained at Howard University Beltsville Campus (HUBC), which is located to the northeast of Washington, DC (39.05N, –76.88W), and is situated in a suburban area with about 5% of the land occupied by buildings. Local emissions of O_3 precursors from Washington, DC, Baltimore, MD as well as those transported from the Ohio Valley and Canada impact the study site (Hu *et al.*, 2011), making it an ideal location for taking observations, and studying a variety of urban air quality processes.

Thompson *et al.* (2013) describe a similar analysis from HUBC and a secondary site near Edgewood, MD (39.4N; 76.3W) during the same period, with the objective to achieve satellite comparisons and contrast the tropospheric O_3 budgets. This paper complements Thompson *et al.* (2013), but focuses on the specific synoptic and mesoscale features that influenced O_3 concentration. Unlike previous studies described at HUBC, where O_3 soundings were launched only during specific poor air quality events (Yorks *et al.*, 2009; Morris *et al.*, 2010), the measurements described here are of unprecedented temporal resolution and obtained over a range of various weather conditions, not only when high O_3 events were forecasted. We specifically examine the transport patterns that help maintain mid and upper tropospheric O_3 maxima, along with parcel trajectories and laminar analyses that characterize the temporal and spatial variability of elevated tropospheric O_3. The application of a temporally dense dataset, however, allows for the examination of both polluted and unpolluted cases, as well as observations of the meteorological mechanisms that vary with both phases of O_3 incidence.

METHODS AND DATA

Atmospheric profiles of O_3 are known to exhibit a layered or "laminar" structure, and it is believed waves such as gravity waves (GW) and Rossby waves (RW) are responsible for the dynamical origins of these layers (Teitelbaum *et al.*, 1996; Pierce and Grant, 1998). For example, laminae associated with RW usually represent downwind advection of a) O_3 pollution and precursors at the various atmospheric levels and b) O_3-rich air from stratospheric/tropospheric exchange (STE). STE is defined as the irreversible transport across the isentropic tropopause, and can represent a significant injection of O_3 and other reactive species into the mid and lower troposphere (Holton *et al.*, 1995). This transport can be triggered by convective systems (timescales as short as a few hours) or baroclinic motion (timescales of days). STE can also occur from tropopause folds in the vicinity of jet stream maxima, cut-off lows, mesoscale convective complexes, thunderstorms, and gravity wave breaking (Stohl *et al.*, 2003). On the other hand, GW normally represents vertical mixing, which means it is associated with convective storms, lightning and boundary layer (BL) mixing. Consequently, it is ideal to distinguish between RW and GW elements to resolve their relative contributions.

The Laminae Identification (LID) method (Thompson *et al.*, 2007a, b; Yorks *et al.*, 2009; Thompson *et al.*, 2010, 2011, 2013) allows an understanding of the dynamical origins of these laminae by exploiting the relationship between O_3 concentration and potential temperature profiles, and it is thus applied here. O_3 profiles were obtained by balloon-borne ozonesondes equipped with electrochemical concentration cell (ECC) sensors that have an accuracy of about 5% in the troposphere (Thompson *et al.*, 2007a; Yorks *et al.*, 2009; Thompson *et al.*, 2013). The O_3 sonde preparations used the procedures described by Komhyr *et al.* (1995) while corresponding pressure, temperature, and relative humidity (PTU) profiles were obtained by coincident Vaisala RS-92 radiosondes. O_3 mixing ratio and potential temperature profiles were interpolated to account for the differences in height resolution from the balloon borne measurements. Small-scale fluctuations were removed by applying a boxcar smoothing method, followed by construction of normalized profiles of both O_3 and potential temperature that were scaled in order to account for the differences in their corresponding vertical gradients (Pierce and Grant, 1998). Then, a moving correlation (r-correlation) was then performed and applied every 5 km at 1 km intervals and results were filtered based on correlation values. Teitelbaum *et al.* (1996) and Pierce and Grant (1998), established that poor correlations (between –0.3 to 0.3) are associated with RWs, while strongly correlated cases ($\geq +0.7$) are associated with GWs (Thompson *et al.*, 2007, 2013). We follow this convention.

These analyses, along with the variation of the tropopause height, were used to help determine whether or not stratospheric intrusion occurred at a given time. O_3 in vertical layers that do not correspond to BL mixing, GW or RW are labeled as background (BG) or residual, meaning that they are associated with air that has aged enough such that its dynamical origins cannot be simply distinguished unless coupled by backtrajectory analysis, or potential vorticity and other tracers.

To further analyze STE cases, folding events were identified using tropopause heights (as shown in Fig. 1), fields of potential temperature (Fig. 2), and relative humidity (RH, Fig. 3) that were derived from sounding data. Since high potential vorticity (PV) values are associated with stratospheric air, sounding data were contrasted against PV derived from European Centre for Medium-range Weather Forecast (ECMWF) ReAnalysis- (ERA)-Interim (Fig. 4). We used this same dataset to evaluate the daily frequency of stratospheric intrusions over the HUBC site. We used ECMWF ERA-Interim PV at 250 mb since we estimated it to be the lower bound for the division of the stratosphere and troposphere. This value was determined by observing which pressure levels have the best match to the tropopause heights observed using the cold point approach on the PTU profiles. Various values of potential vorticity units or PVU ($1\ PVU = 10^{-6} m^2 s^{-1} K\ kg^{-1}$) are used to indicate the

separation between stratosphere and troposphere, but for the purpose of this study, we use 1.5 PVU (Holton, 1985; Stohl *et al.*, 2003; Chen, 2005; Kim *et al.*, 2008) as long as these fields match the condition of RH ≤ 20%, which is established as a condition for stratospheric intrusion. Events satisfying the criteria are shown on Fig. 5. The laminae distribution is embedded on Fig. 6 (GW laminae) and Fig. 7 (RW).

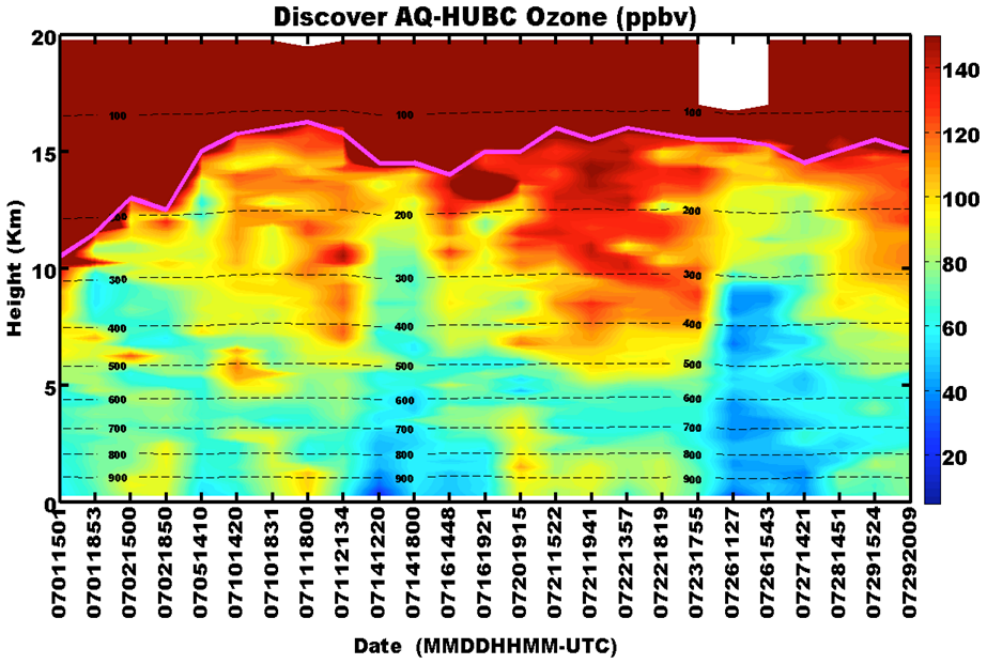

Fig. 1. O_3 mixing ratio contour (in ppbv) from 25 daytime O_3 sonde measurements collected between 1 and 29 July 2011 at HUBC Maryland during the DISCOVER-AQ campaign. The x-axis indicates the date and launch time in UTC (e.g., MMDDHHMM), which also matches the aircraft over-flight of HUBC. The data (e.g., time axis) are rendered sequential in order of time of launch but not linear in time to emphasize the changes in the tropospheric O_3 structure throughout the campaign. Magenta colored line represents the tropopause height, which was obtained applying the World Meteorological Organization (WMO) definition. Pressure levels are overlaid.

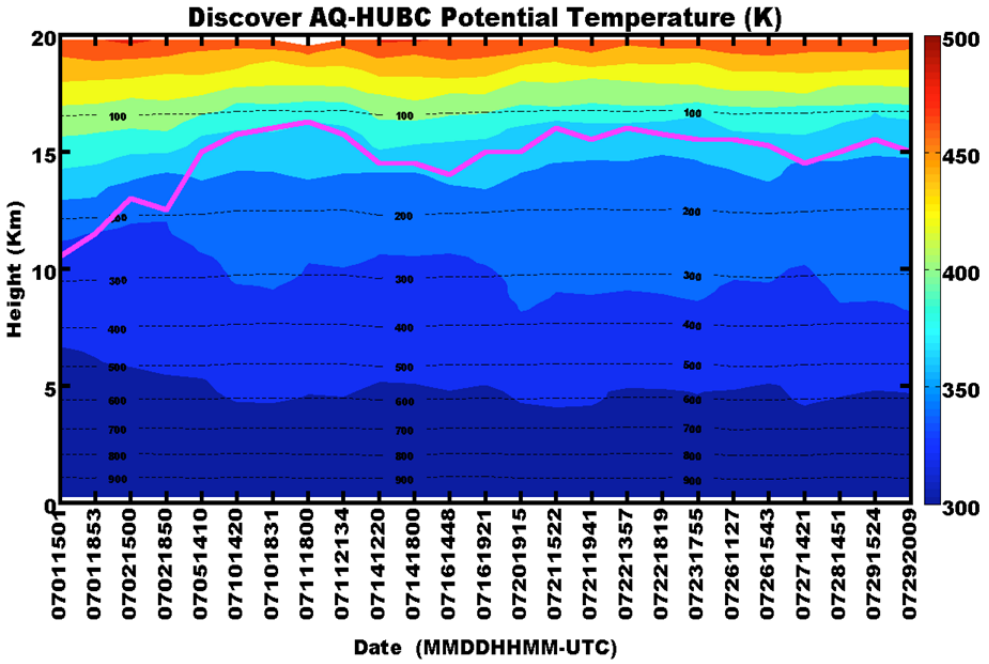

Fig. 2. Potential temperature as derived from O_3 sonde data (in Kelvin) during July 2011 at HUBC Maryland. As in Fig. 1, the magenta colored dots represent the thermal tropopause and pressure levels (in hPa) are superimposed.

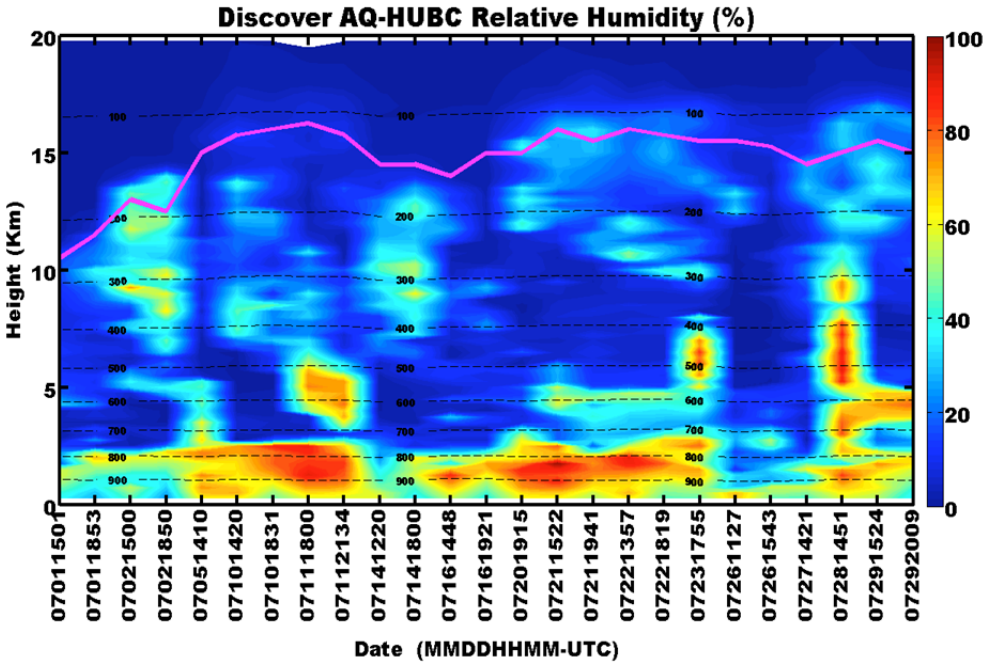

Fig. 3. Same as previous figures, but for Relative Humidity (%).

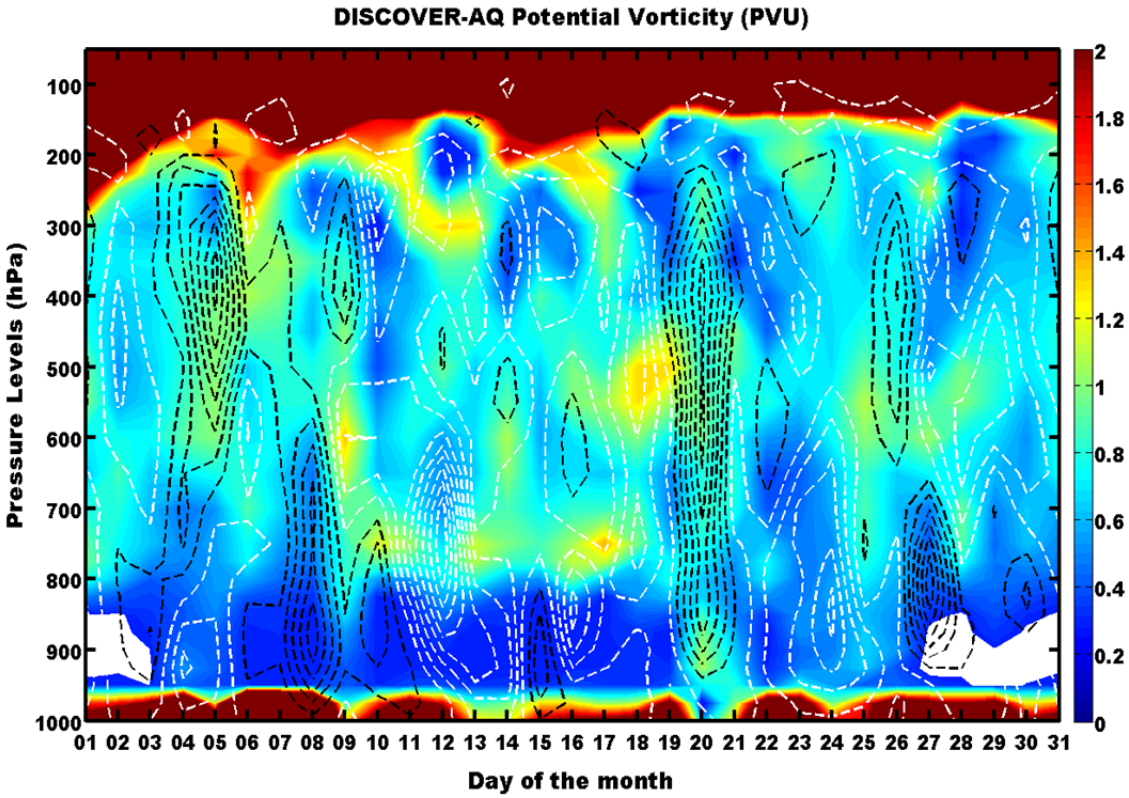

Fig. 4. Reanalysis using PV fields from ECMWF ERA-Interim with superimposed vertical velocity, also derived from ERA-Interim. Black contours denote areas of sinking motion (negative vertical velocity), while white contours denote rising motion. PV is in PV units (PVU).

RESULTS AND DISCUSSIONS

Fig. 1 shows the O_3 mixing ratio (in ppbv) contour from soundings collected between 1 and 29 July 2011 at HUBC at an interval of 10 ppbv and ranging from 5 to 150 ppbv. Twenty-five daytime launches are shown, most of them coinciding with times when a NASA P-3 aircraft was spiraling over the HUBC site. Because of the codependency

with the airplane overpasses, the data were gathered in a non-regular frequency (generally two sondes per flight day, but not necessarily during consecutive days). However, the figure includes all 25 launches consecutively to emphasize the changes in the tropospheric O_3 structure throughout the campaign. Comparisons of HUBC sondes and the P-3 below 2 km are in good agreement (Thompson *et al.*, 2013).

Most O_3 soundings reached altitudes of 32 km or above.

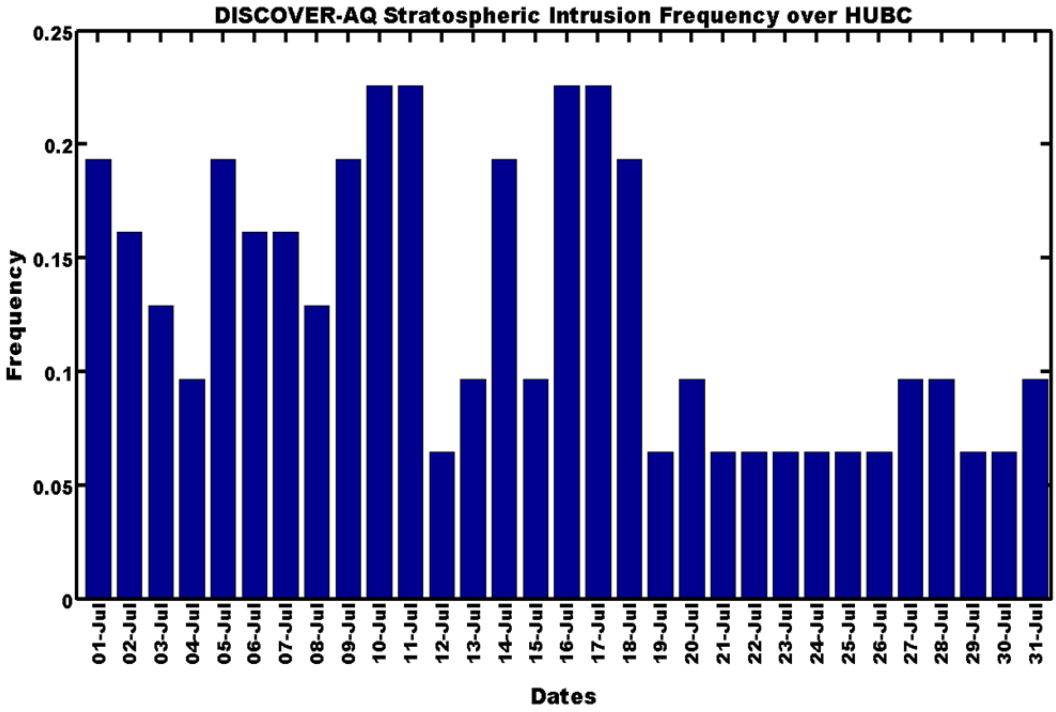

Fig. 5. Daily frequencies of stratospheric intrusions over the DC area (and HUBC) using ECMWF ERA-Interim reanalysis PV and RH data over the month of July 2011. A stratospheric air intrusion is defined by PV greater than 1.5 PVU and RH less than 20%. An event satisfying the criteria is counted and divided by the total number of days in the campaign.

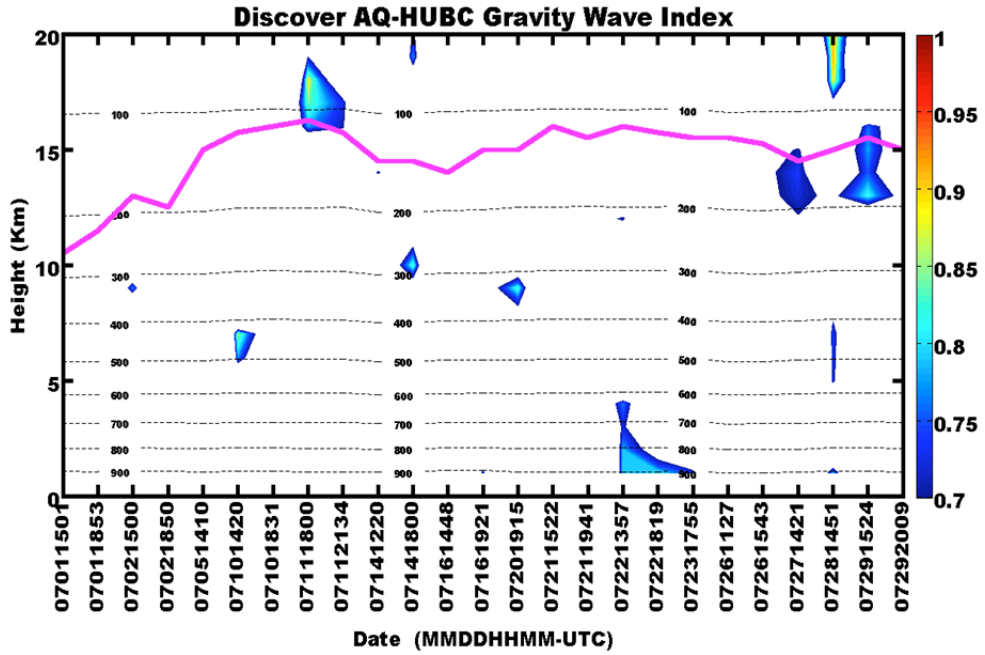

Fig. 6. Distribution of the GW laminae over HUBC during DISCOVER-AQ as obtained by applying the Pierce and Teitelbaum laminae (PT) analysis to the O_3 profiles. 5 km vertical correlations are applied to the normalized profiles within 1 km increments. Panel shows correlations of 0.7 and above which are associated with GW and are denoted by the shaded areas. The contours represent line of equivalent potential temperature.

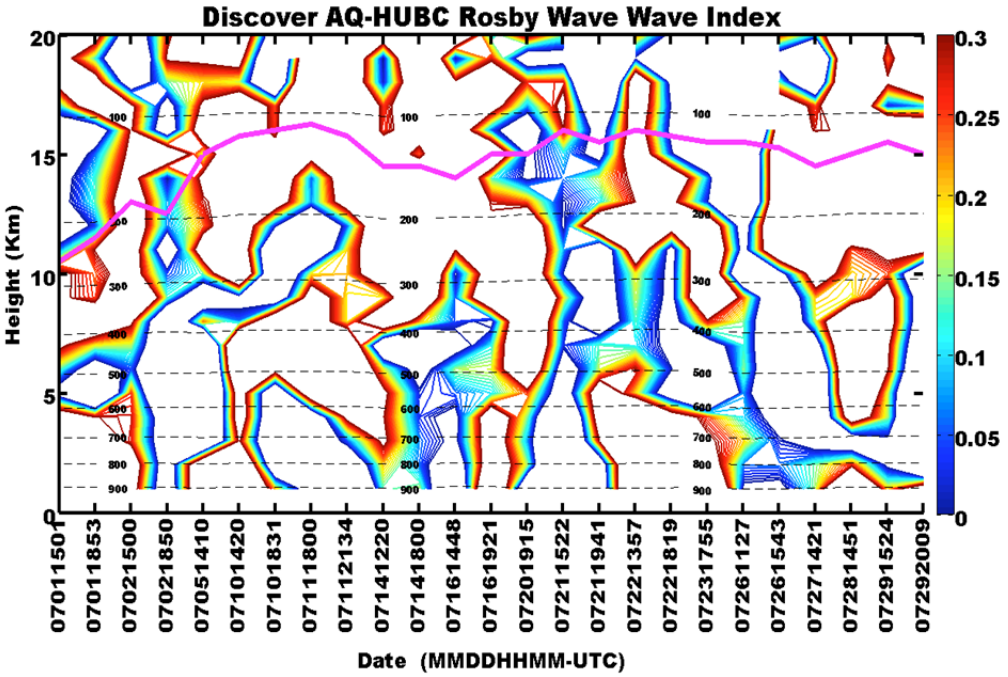

Fig. 7. Same as Fig. 6, but for the RW laminae distribution. Note the shaded regions correspond to the absolute value for correlations between 0 to +0.3 (instead of –0.3 to 0.3).

However, data are shown from the surface up to 20 km in order to highlight O_3 interactions between the troposphere and stratosphere. Here, we employ a traditional definition of the tropopause, identified as the lowest level at which the lapse rate decreases to 2 °C km^{-1} or less (World Meteorological Organization–WMO), which is represented by the magenta line in Fig. 1. Using this method, the average tropopause height over all launches was 14.75 km, corresponding to a mean potential temperature surface of 360 K. Because the thermal distinction between the troposphere and stratosphere sometimes corresponds to an atmospheric layer rather than just a single point, we follow an analogue procedure used by Thompson *et al.* (2003, 2007a, b, c, 2011, 2013), in which a tropopause transitional layer (TL) is broadly defined. For the purposes of this study, the TL corresponds to the region between 12–16 km. What we denote as the mid troposphere lies between 5–12 km and the lower troposphere is defined as anything below 5 km. The BL height was averaged at 1 km for all launches and the calculated percentages correspond to the total laminae found within the surface to the BL height. We also defined the free troposphere as a layer comprised between 1 and 12 km.

At the surface level, four events occurred in which O_3 concentrations reached or exceeded 76 ppbv (Fig. 1), a value that serves as an approximate threshold for poor air quality conditions. O_3 concentrations between 5–10 km for the HUBC site normally average between 70 to 100 ppbv. These data, however, show several instances in which O_3 concentrations significantly exceeded this range, reaching values between 90 and 160 ppbv. Each case of O_3 enhancement was followed by reductions of tropospheric O_3 at varying tropospheric depths, which were primarily triggered by frontal passages through the region (05 July 10–14 July, 16 July, 20–22 July). Although our primary focus falls on meteorological causes associated with O_3 enhancement in the mid-upper troposphere, we also explore the meteorological nature of anomalously low events, and particularly a substantial reduction of column O_3 on 26 July. The discussion of these study cases is found below.

Mean Statistics

Fig. 8 complements Fig. 1, as it shows the integrated tropospheric O_3 (ITO_3) between 1–20 km, but in Dobson Units (DU) for each of the 25 obtained profiles. The highest ITO_3 corresponds to the 1501 UTC (11:01 am, local Eastern Time) 01 July sounding, with values exceeding 60 DU, and the lowest on 1127 UTC (7:27 am, local Eastern Time) on 26 July when ITO_3 values barely reached 20 DU. Fig. 8 also displays information about the contribution of each laminae based on the definitions of GW, RW and BG O_3 presented on the previous section.

BG O_3 is the greatest contributor to the column-integrated O_3 budget (Fig. 8) followed by RW, accounting for 41.7% and 31.7% of the tropospheric column O_3 during the entire observation period. On the other hand, GW-induced O_3 is the least influential mechanism, present only in 14 out of 25 of the profiles (Fig. 8) and 11.7% of the total budget. BL processes account for as much as 14.9% of the total budget. These numbers are in agreement with observations described by Yorks *et al.* (2009) who conducted studies at our same site during the summers of 2004–2007. They are also in agreement with Thompson *et al.* (2013), in which they found the corresponding budgets for the HUBC site as 18.9% for BL, 13.1% for GW, 27.3% for RW and 40.7% for background. Even though the methodology to calculate

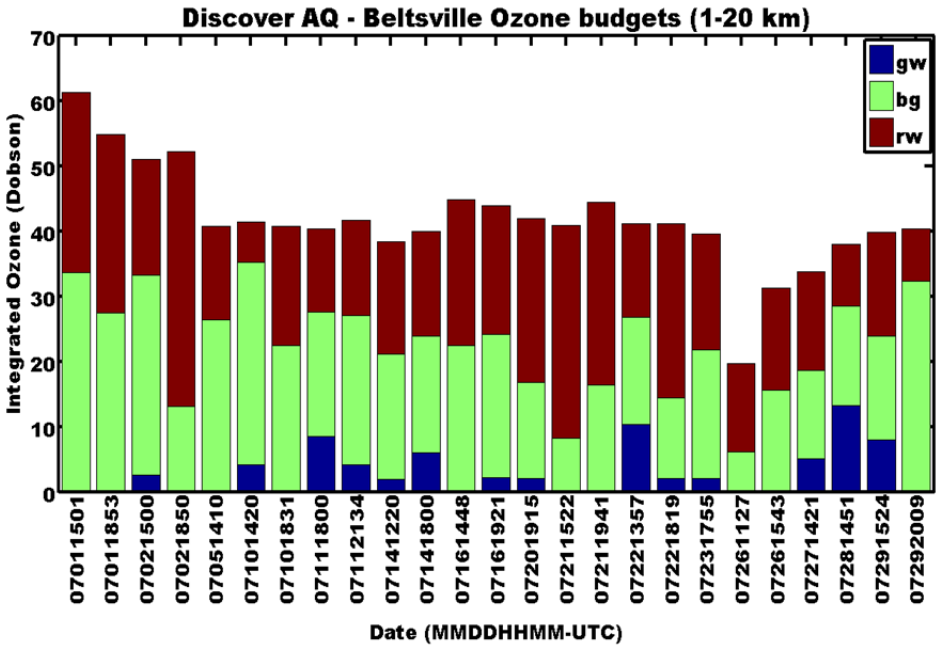

Fig. 8. Integrated tropospheric O_3 (in Dobson units) between 1–20 km as obtained from daytime O_3 sonde measurements at HUBC Maryland during the DISCOVER-AQ campaign. Each bar also shows the contribution of each of the mechanisms responsible for tropospheric O_3 enhancement. It is noticeable how the BG and RW laminae are by far dominate most of the budget, while the GW contribution is minimal and observed in 14 of the 25 the profiles.

the budgets is similar for both studies, some differences arise due to how the BL height and tropopause height are defined. STE was the most influential mechanism influencing total column concentrations by virtue of both RW and GW, though we note the possibility of the influence transport from polluted areas may play, which we will discuss in more detail in the subsequent sections.

Meteorology of Period 1: 01–05 July

On 01–02 July the Mid-Atlantic region was dominated by the influence of anticyclonic flow at the surface and an upper-level ridge. This anticyclone followed an occluded surface low that was moving through eastern Canada, carrying with it a warm front that stretched southward across Maryland and bringing stagnant winds with relatively dry conditions. These would imply that corresponding high O_3 concentrations were mainly the result of local pollution. Fig. 1 depicts the evolution of the first elevated surface O_3 event of the month, which reached its peak on 02 July. The atmospheric sounding data reveal peak O_3 concentrations greater than 90 ppbv within the first 2 km.

Elevated O_3 concentrations were also observed above 6 km on 01 July (Fig. 1). Potential temperature contours (Fig. 2) show that tropopause did not strictly follow the 360 K isentrope on these first two days. Coincidentally, Fig. 4 shows how PV values increases between the 300–200 hPa levels and were accompanied by sinking motion (black contour lines). This scenario suggests that a STE occurred that was triggered by a tropospheric fold, specifically driven by RW breaking (Figs. 5, 7 and 8) and resulting in the transport of O_3-rich air into the upper and mid troposphere. The corresponding profiles obtained from soundings on 01 July, show that the column was mostly dominated by RW and BG induced O_3, which correlate with very low levels of RH. Aircraft tracers – mainly CO and the collective of oxidized forms of nitrogen or NO_y (NO, NO_2, nitric acid (HNO_3), and organic nitrates), support this interpretation (Thompson *et al.*, 2013). STE events associated with tropopause folds typically occur west of an upper-level trough, and are enhanced by the presence of a jet (Shi *et al.*, 2012). The 250 hPa analysis for this day (not shown) demonstrates that Maryland sat along the western edge of an upper-level trough and is also directly under a jet streak.

While surface O_3 levels were greater on 02 July, mid-tropospheric O_3 (6.5–10 km) plummeted from maximum values of 100 ppbv to 60 ppbv, except for a sharp increase in O_3 at the 6 km level that is persistent both days and associated with low RH and RW-induced laminae. Evidence of subsidence within the column is shown on Fig. 4 (black contours) during both days, especially at upper levels, consistent with a folding event. The 1500 UTC (11:00 am, local Eastern Time) sounding on 02 July shows O_3 in the 9–13 km region as mostly background, with highly variable RH profiles sometimes exceeding 50% within 8 to nearly 15 km.

During the afternoon of 03 July, a warm front passed through the region, triggering a local microburst that was followed by a cold frontal passage on 04 July. The front produced showers and severe thunderstorms over Washington, DC, Maryland and portions of Virginia, with wind gusts on the order of 60 mph as well as large hail. The National Weather Service (NWS) high resolution S-band Doppler Next Generation Radar (NEXRAD, Fig. 9),

depicted a period of heavy precipitation over HUBC that lasted over 40 minutes on 03 July (2207 through 2248 UTC, 6:07–6:48 pm, local Eastern Time), followed by periods of intermittent light showers over the following two days. These conditions resulted in a surface "clean-up" that can be observed from the 05 July O_3 sounding (Fig. 1). On the other hand, Fig. 4 shows a corresponding increase in PV above 650-hPa on 05 July that was accompanied by subsiding air, while Fig. 5 shows an increase in STE potential on 04–05 July that may suggest a STE event. The derived tropopause height (Fig. 2) also does not follow the 360 K surface on 05 July, indicating a possible tropospheric fold.

Though tropospheric O_3 enhancement for this period was mostly the result of STE, horizontal transport of O_3 precursors may have also contributed to mid-tropospheric O_3 enhancement (5–10 km) on 05 July. Enhanced atmospheric attenuation due to fires and smoke were reported over a substantial portion of the south-central Canadian plains, as well as western states such as New Mexico and Colorado. Forty-eight to seventy-two hour back trajectories

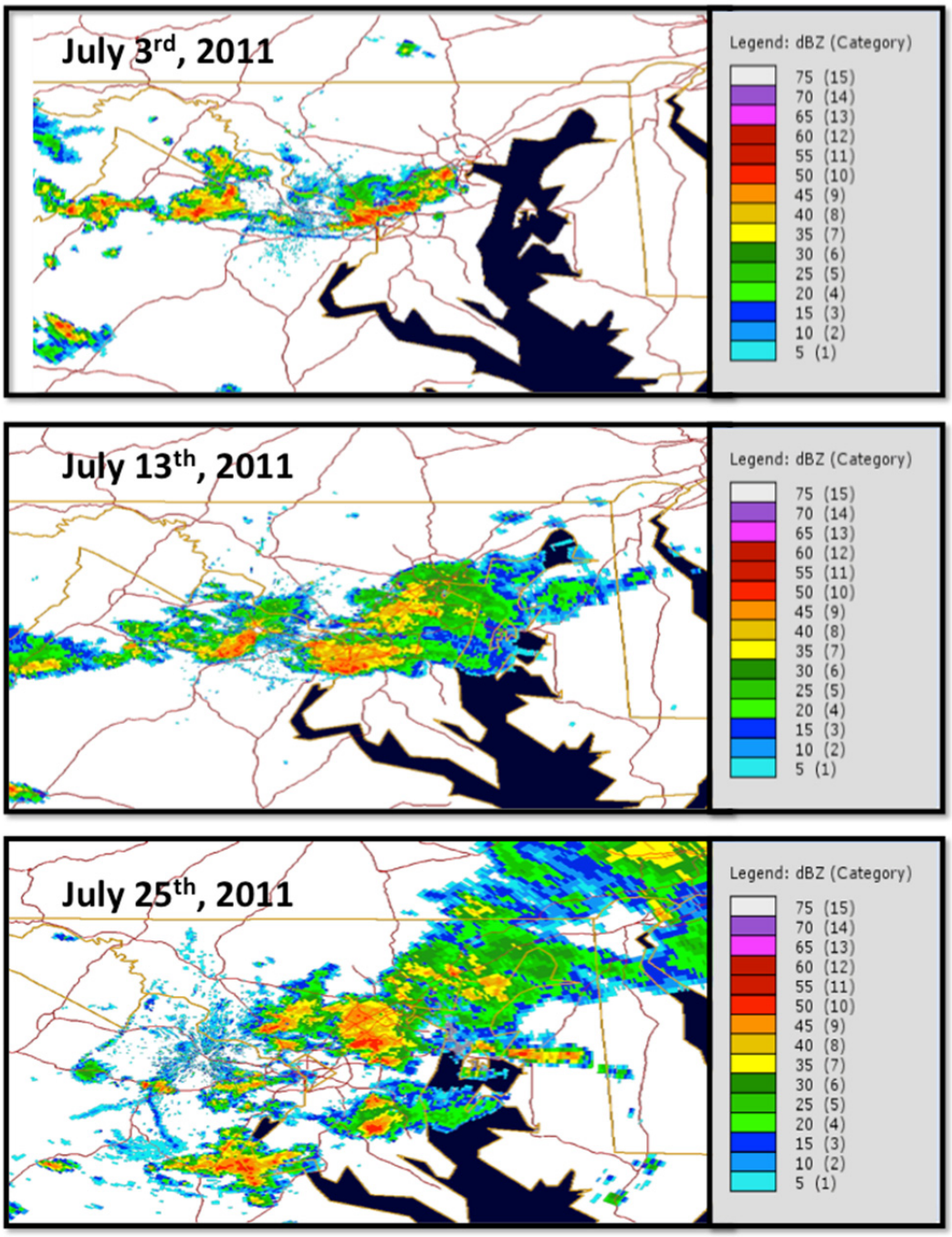

Fig. 9. (Above): shows NOAA Next Generation Radar (NEXRAD) images for the 2225 UTC (6:25 pm, local) 03 July , 1923 UTC (3:23 pm, local) 13 July, and 1925 UTC (3:25 pm, local) 25 July We can observe the difference on the spatial extent and relative strength of all three storms as they were impacting the HUBC, MD area.

(supplemental materials) for 04 July show air being advected from New Mexico and Arizona. Trajectories beginning 05 July (supplemental materials) show air masses originating closer to fires in Saskatchewan and Alberta.

Meteorology of Period 2: 06–16 July

Good surface air quality prevailed around the Maryland region, due to the presence of a stationary cold front 07–08 July. Late in the day on 08 July, a storm developed producing the greatest precipitation amounts recorded at the site during the campaign. Despite this, mid and upper-level winds were steering O_3 precursors (smoke) from Canadian fires occurring in Ontario towards the Great Lakes region. Of particular interest, were large fires south of Reindeer Lake (57.5°N, 102.0°W) on 07–08 July, which moved southeast toward Maryland arriving 10–11 July. We analyzed the 532 nm backscatter signal obtained by the Cloud-Aerosol Lidar and Infrared Pathfinder Satellite Observation (CALIPSO) satellite, corresponding to these cases and could observe two strong signals: one located close to Saskatchewan, Canada (between 65.91N, 100.59W–71.53N, 103.73W) that spreads between 4–9 km, and a second one close to the Great Lakes Region (54N, 92W) between 8–10 km (not shown). At the same time, fires over the USA continued, most notably in Georgia and Northwest New Mexico, around Las Conchas and Pacheco.

On 10 July, a high-pressure system and a large-scale upper-level ridge covered most Continental United States (CONUS), bringing clear conditions and calm winds out of the southwest. The Bermuda High was pushed to the east as a front moved off the coast of the United States. These conditions, which are known to be conducive to high surface O_3 in Maryland, enabled the second high surface O_3 episode of the month. Atmospheric soundings collected on 10–11 July at HUBC during the mid-morning and afternoon show O_3 peak levels ranging between 88 and 105 ppbv between the surface and the BL (Fig. 1). In the mid-troposphere, they exceeded 150 ppbv near 10 km on 11 July (Fig. 1). A very dry layer developed between 3–6 km, coupled with a slight temperature inversion near 3 km that persisted through 11 July. Analysis of the individual laminae profiles corresponding to the on the 1400 UTC (10:00 am, local) 10 July sounding (complemented by Figs. 7–8), show that the column was mostly dominated by background O_3. However, a GW-induced layer located between 6–7 km, with values exceeding 100 ppbv, was observed that gave way by the 1800 UTC (2:00 pm, local) radio/ozonesonde launch to more RW-dominant conditions. Both soundings show a mixture of RW and background O_3 throughout the column with some GW filaments, but the highest O_3 concentrations (O_3 exceeded 100 ppbv at mid and upper levels) were coupled with RW activity.

STE was likely the principal mechanism for O_3 enhancement in the mid and upper levels on 10–11 July. Fig. 4 shows an increase in PV content between 09–10 July, which is accompanied by subsiding (09 July) and then rising (10 July) motion respectively. These high PV fields in the mid-troposphere (Fig. 4) may have been triggered by the previous thunderstorm activity. Fig. 5 shows, however, that some of the highest STE frequencies for the entire dataset correspond to 10–11 July. Fig. 4 also shows a reduction in PV during 11 July, when mid-upper air values of O_3 range from 100 ppbv between 6–10 km during the 21 UTC (5:00 pm, local) launch. The impact of the fires and transport on 7–8 July cannot be fully ruled out as precursor elements. However, a P-3 aircraft flown concurrently during the NASA DISCOVER-AQ did not capture relevant smoke concentrations at that altitude. Figs. 10(a)–10(b) show 72 hour National Oceanic and Atmospheric Administration (NOAA) Hybrid Single Particle Lagrangian Integrated Trajectory (HYSPLIT) model air mass back trajectories between 5–10 km, coinciding with selected launches on 11–10 July. These originate from both Canada and the midwestern U.S. respectively, which could imply injection of O_3 or O_3 precursors during this time frame.

After the precipitation event on 11 July, smoke transport from fires in the Mississippi Valley region was observed at HUBC. Although ozonesonde data was not collected on 12 July, a "code orange" urban alert (unhealthy for sensitive groups) was issued in Maryland and Washington, DC that afternoon, with air quality levels improving during the evening. On 13 July, a cold front moved through Maryland bringing showers and thunderstorms again to the region. Precipitation from this system was more widespread than in the previous events (Fig. 9), and also was longer lived with heavier rains.

The cold fronts on 11 and 13 July served to clean out much of the eastern seaboard, allowing a return to moderate levels of surface air quality in regions previously affected by fires. However on 14 July, fire activity picked up again. Large wildfires in New Mexico and the surrounding area, as well as the numerous wildfires in the Ontario and Manitoba produced dense smoke and high aerosol optical depth (AOD) values observed by the MODIS Terra (not shown). Poor air quality was forecasted for Maryland on 14 July, yet surface levels remained between the healthy and moderate range. At HUBC, O_3 sonde operations resumed on this day and soundings at 12 and 18 UTC (8:00 and 2:00 pm local Eastern Time) showed peak surface O_3 concentrations of 49 ppbv and 58 ppbv, respectively. Similarly, O_3 levels between 5–10 km remained relatively low (max around 70 ppbv) compared with measured values observed on 11–12 July. There is evidence of some GW-induced laminae (Fig. 6), but Fig. 4 shows a small area of PV intruding close to 250 hPa, which may indicate small Rossby Wave Breaking (RWB) and a possible short-lived stratospheric intrusion that was not as deep or extensive compared with all other cases. STE frequency increased on the 14 July, lasting through 17 July (Fig. 5), with alternating regions of air ascent and subsidence (Fig. 4) throughout the column.

Surface O_3 levels remained low through 20 July. However beginning with 16 July, sounding observations showed a substantial O_3 increase within the 6–12 km layer. PV reanalysis (Fig. 4) shows some evidence of stratospheric injected air (below the 250 hPA level), despite of the lack of substantial variation in the 360 K-isentrope heights. The upper levels were dominated primarily by ascending air (white contours on Fig. 4), which may have hindered

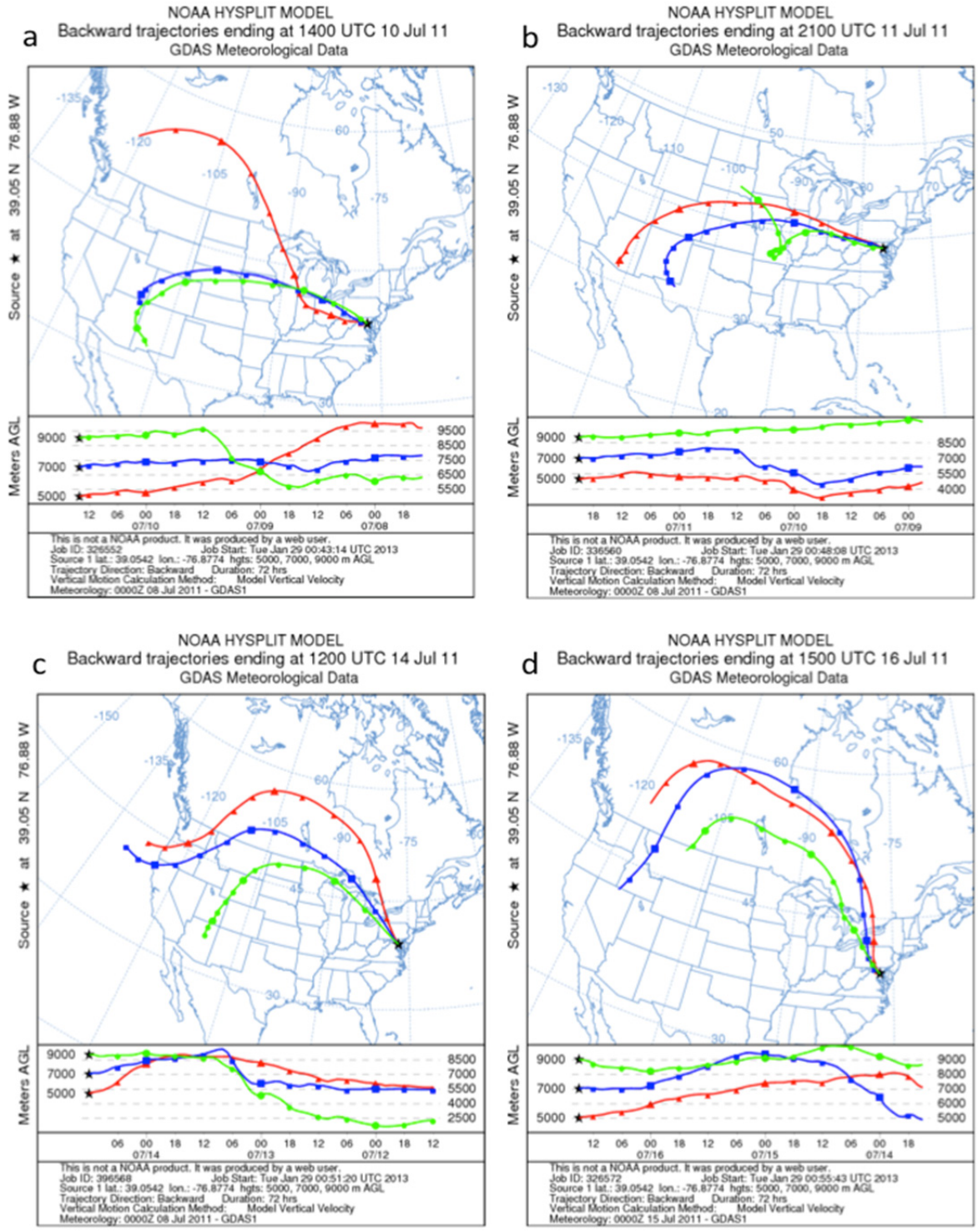

Fig. 10. NOAA HYSPLIT Back trajectories, corresponding to select launches between 10–16 July. These show runs at 5, 7 and 9 km.

vertical transport to the surface. Yet, areas in which the O_3 mixing ratio exceeds 110 ppbv (around 10.5 km) are seen, in contrast with the less than 70 ppbv measurements made at the same altitude on 14 July.

Meteorology of Period 3: 17–29 July

Beginning 18 July, poor air quality conditions at the surface returned to the Mid-Atlantic region. Smoke transport from active fires observed in northern Ontario and Quebec was also taking place. An anticyclone centered over the region brought southerly winds off the Atlantic while increasing column moisture levels. A very strong upper-level ridge was shifting eastward strengthening southwesterly flow, adding another ingredient to the poor air quality recipe.

From 20–24 July, the Mid-Atlantic experienced the national record-breaking heat wave in which 1,966 daily high maximum temperature records were broken or tied (Payne *et al.*, 2014). Smoke from the Canadian fires had also drifted towards the Northeast US, while fires in central and eastern Canada, mainly Manitoba and Ontario, continued advecting very dense plumes towards the Northeast and Mid-Atlantic states.

Surface O_3 concentrations increased dramatically around the region, with some stations reporting an unhealthy air quality rating (code red). At the HUBC site, O_3 levels did not increase enough to reach a code red. Nevertheless, concentrations above 80 ppbv were observed during four consecutive days within the BL and soundings measured up to 110 ppbv during the afternoon on 20 July from 0–2 km. Yet, there was very strong mid to upper tropospheric enhancement in O_3 concentrations. Fig. 4 does show evidence of moderate PV air along the column during 20 July, though not as markedly as seen in the cases previously addressed. PV levels remained low along the column and did not pick up until after 23 July. Fig. 5 also shows lower than average STE frequencies for profiles obtained between 21–26 June.

At 1400 UTC (2:00 pm, local Eastern Time) on 20 July, most of the O_3 within 5–12 km is of background origin (Fig. 8). Four additional soundings were obtained between the 21–22 June, depicting an alternating trend between background O_3 and RW-induced O_3-controlled profiles. Figs. 11(a), 11(b) and 11(c) show HYSPLIT back trajectories during this time period. The analysis shows air masses that had been advected through Saskatchewan (Fig. 11(a)) and Ohio Valley (Fig. 11(b)), prior to arrival at HUBC on 20–21 June, respectively. Transport likely played a more significant role than STE and BL processes during this event, though not necessarily from O_3 precursors due to fire activity (which would have been the case for air masses advected from Canada). Instead, areas characterized by continuous production of anthropogenic pollutants (Ohio Valley region) were a likelier stimulant.

Air quality improved substantially after 23 July. A stationary front was cast over Maryland for most of that day producing showers and thunderstorms. Heavy rain produced flash flooding and was accompanied by damaging winds near the DC area. Low levels of O_3 concentrations (not exceeding 70 ppbv) prevailed at heights below 10 km in the wake of the frontal passage and precipitation event. As can be noted in Fig. 1 and Fig. 8, tropospheric column O_3 was reduced extensively compared with all of the other cases. This same behavior can be observed in the O_3 column data obtained at the Edgewood ground station (Thompson *et al.*, 2013), which is north of HUBC. Calculations of integrated column O_3 (in Dobson units or DU) from the surface up to 10 km show 23.0 DU on 1941 UTC (3:41 pm) 21 July, followed by a dramatic decrease of nearly 70% on 26 July (12.2 DU), building up further by 27 July.

Previous research (Hu *et al.*, 2010) has examined the effects of deep, tropical convection on concentrations of O_3 throughout the troposphere. They observed that deep convection reduced O_3 concentrations in the upper troposphere (12–15 km) by 50% and enhanced it by 39% in the lower 2 km. At HUBC, representative of a mid-latitude atmosphere, a number of meteorological processes contributed along with the associated precipitation and dynamics from the storm, including a Canadian airflow "blockage" that was formed due to the interaction of the frontal system and a high pressure that developed over the north central USA. Fig. 12 shows NOAA's Weather Prediction Center (WPC) surface pressure and precipitation maps for July 24–July 27. Following the stationary front on 25 July, a cold front proceeding from the Northwest also approached the region. The atmosphere was already very moist due to the precipitation associated with the stationary front, with relative humidity values above 70% up to 700 mb (not shown), yet, on the next day (26 July), another cold front arrived from the northwest accompanied by an outflow boundary along the Maryland/Pennsylvania border as Maryland sat at the edge of an upper-level trough that was moving over New England. The Bermuda High had shifted slightly eastward and was obstructed near the east coast by a front stretching off of a low-pressure system moving out of Canada, bringing north/northwest winds into the Mid-Atlantic. During the frontal passages on 25 July, an area of high pressure lingered in the north central USA, covering portions of both USA and Canada. This area moved eastward until 27 July, thus heavily influencing air flows. The position of the high --- northwest of the region --- brought clockwise circulation and helped to steer air masses proceeding from the northern regions. Thus, air masses during this period were advected more from the north-central United States, where air quality levels were ranging between good and moderate. We can observe this change in air masses comparing Figs. 11(a), 11(b) and 11(c) (all polluted cases) with the particular case of Fig. 11(d) (air mass proceeding from cleaner areas, or where fire activity was at minimum during this period). This air mass shift is evident in both back trajectory and in-situ data at HUBC (Payne *et al.*, 2014). Sounding data from the NWS-Sterling was used to look at the horizontal wind profiles corresponding to the precipitation events during the DISCOVER-AQ campaign, when no launches were performed at the HUBC site. It seems that from all storms, the system on July 25 exhibited the weakest horizontal winds up to the 12 km level. Consequently, O_3 concentration around the mid-troposphere remained low compared with cases in which polluted air mass advection was present.

By 27 July, the cold front had passed through Maryland and was followed by an area of high surface pressure accompanied by an upper-level ridge. During this same day, light to moderate smoke was observed from southern Maryland through northern South Carolina as a consequence of the North Point wildfire in Wyoming and fires in Canada. Fig. 5 shows that STE frequency increases for 27–28 July. By 28 July, surface air quality had deteriorated in the east coast, where particulate matter (PM) 2.5 and O_3 reached moderate and unhealthy levels. O_3 increased during the afternoon in the Mid-Atlantic, while fires and smoke from Quebec continued to be reported. The effect

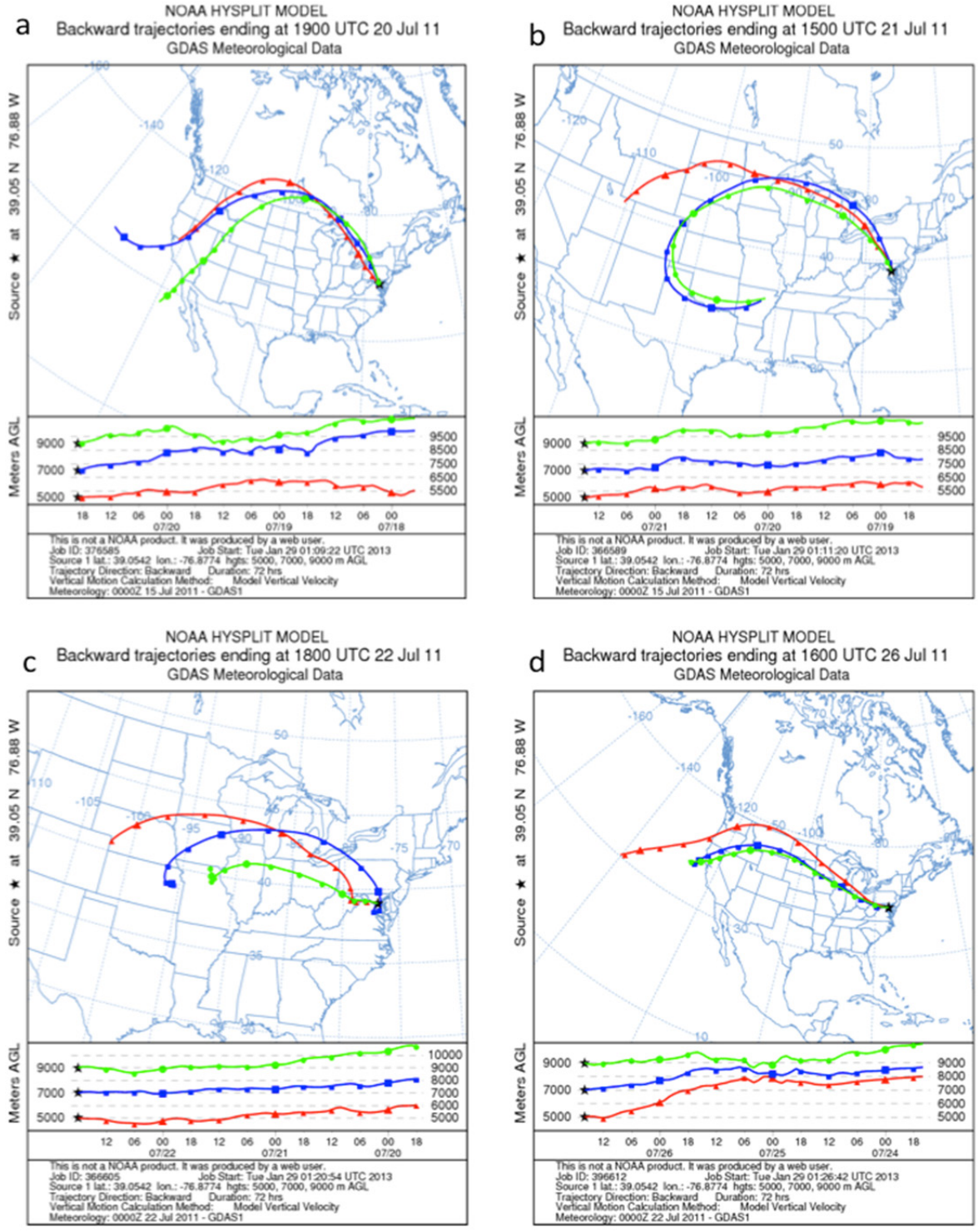

Fig. 11. NOAA HYSPLIT Back trajectories, for the record-breaking heat wave (20–22 July corresponding to panels a, b and c) and column clean-up event (26 July).

of these last fires, along with a building high-pressure system and increasing temperatures is observed in Fig. 1, as O_3 increased again both in the lower and mid-upper tropospheric levels after the cleanup event. These were the last soundings conducted during the campaign. Another heat wave hit the east by the end of this period, with temperatures exceeding 100°F (37.8°C) in most places in the Mid-Atlantic. O_3 levels in the region once again ranged from moderate to unhealthy.

At this point, it is noteworthy to mention that Figs. 6 and 8 and show fragments of GW between 8 and 10 km and one above 12 km during the last portion of the campaign. GW lamina is normally associated with regional convection and lightning. Although the impacts of lightning are not

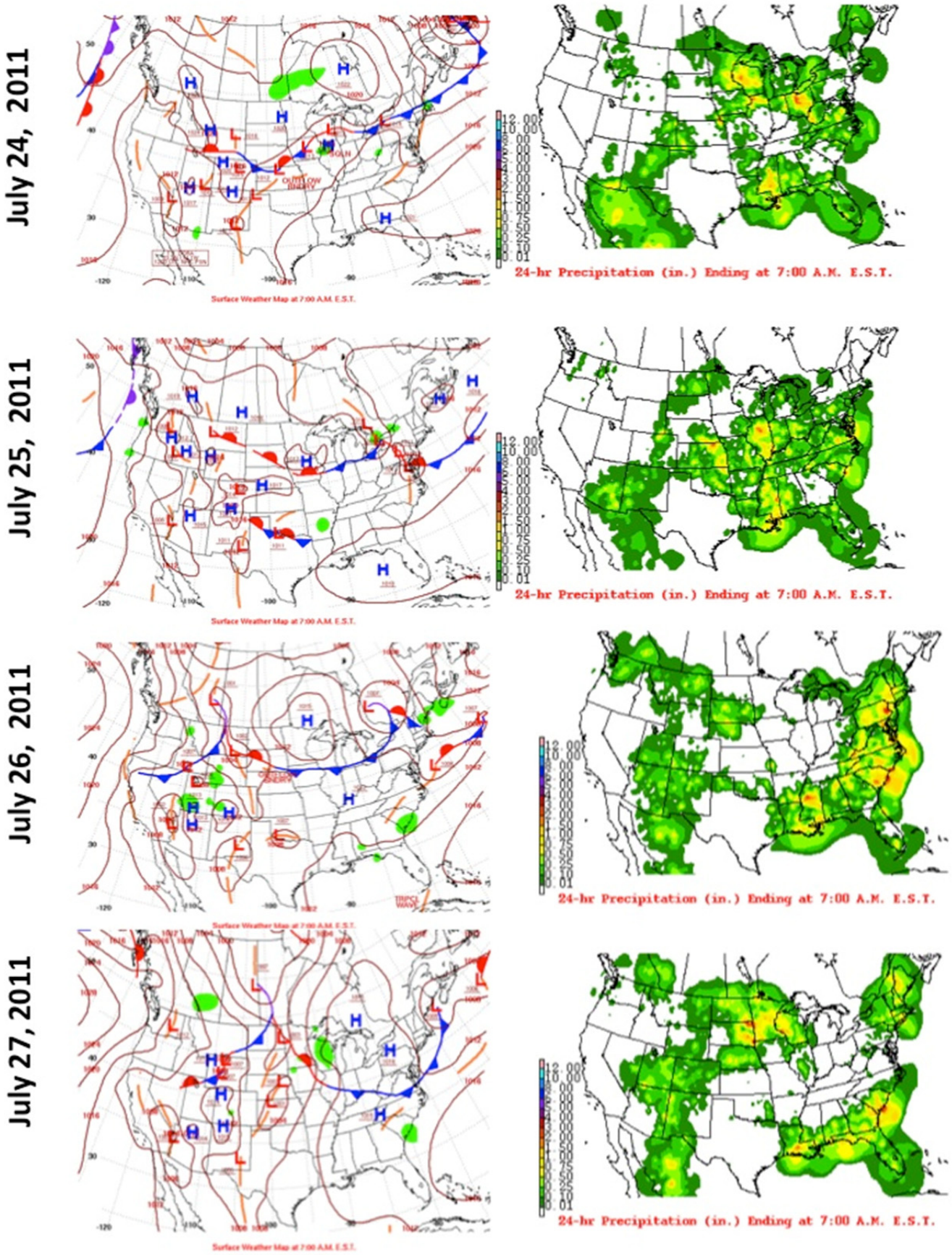

Fig. 12. NOAA Weather Prediction Center (WPC) surface pressure and precipitation maps corresponding to the O_3 depletion scenario between 24–27 July.

fully explored in this publication, it is noteworthy to mention that Thompson *et al.* (2007a) pointed out that a complex mixture of stratospheric, lightning, and long-range transport influences the O_3 variability in the DC-area. This in itself is a future area of study.

SUMMARY

Here, we described the synoptic and mesoscale meteorological drivers influencing O_3 profile variability in the Washington, DC vicinity during summer 2011. We applied the LID method (Thompson *et al.*, 2007a, b; Yorks *et al.*, 2009, Thompson *et al.*, 2010, 2011, 2013), which allows to resolve the relative contribution from planetary waves in the atmospheric column ozone. Specifically, we highlight how RW and GW are responsible to originate and maintain mid and upper tropospheric O_3 maxima through downwind advection of O_3 pollution and precursors at the various atmospheric levels and O_3-rich air from STE.

The mean statistics derived from the laminar analysis show that background O_3 tends to dominate the laminar budget, followed by RW, accounting for 41.7% and 31.7% of the tropospheric column O_3, respectively. These changes resulted primarily from stratospheric intrusion. However, there was a strong influence from advection of pollutants and STE produced at other locations. The BL dynamics and photochemistry accounted for 14.9%, while GW contributed with 11.7% of the total budget. These results are similar to the ones obtained by Thompson *et al.* (2013).

There were four periods of mid-upper tropospheric enhancement over HUBC during July 2011, which are primarily dominated by STE. Most of the variability was triggered by convective systems, baroclinic motion and tropopause folds in the vicinity of jet stream maxima. The first was an intrusion case on 01–02 July, caused by a tropopause fold over Maryland in the presence of a jet streak and an upper level trough. We showed that for the subsequent cases (05 July 10–14 July, 16 July, 20–22 July) there is the possibility that horizontal transport may have contributed to O_3 enhancement. Even though coincident aircraft spirals during DISCOVER-AQ show low concentrations of CO and smoke at those levels, we do not discard the possibility of stratospheric air or pollution being transported from upwind, especially in cases like 20–22 July, when the ECMWF reanalysis does not show strong evidence of high PV air at the upper levels. The dynamical processes associated with frontal passages and changes in air mass characteristics also contributed to reductions in O_3 levels not only at the surface levels but also throughout the column. Example of this was the dramatic decrease of nearly 70% in free tropospheric ozone on 26 July.

We have demonstrated how weather can serve as the primary driver for transport of O_3 and its precursors. Nevertheless, monitoring and understanding of weather conditions should not be limited to just surface as downward transport of air from the entire atmospheric column can contribute before, during and after poor air quality events. Therefore, vertical characterization of O_3 (and aerosol) profiles from surface to the lower stratosphere, combined with knowledge of the prevalent atmospheric conditions is necessary and should not be decoupled from chemistry.

ACKNOWLEDGMENTS

Author MO wants to acknowledge the American Society for Engineering Excellence (ASEE) as well as the Naval Research Laboratory for their support on this publication. The data collection for used here was possible in part by the support of the National Aeronautics and Space Administration (NASA) University Research Center grant NNX08BA42A and the National Oceanic and Atmospheric Administration (NOAA) Center for Atmospheric Sciences (NOAA-CAS) at Howard University, through the NOAA's Educational Partnership Program Cooperative agreement NA11SEC4810003.

REFERENCES

Aneja, V.P., Mathur, R., Arya, S.P., Li, Y., Murray, G.C. and Manuszak, T.L. (2000). Coupling the vertical distribution of ozone in the atmospheric boundary layer. *Environ. Sci. Technol.* 34: 2324–2329.

Bell, M.L., McDermott, A., Zeger, S.L., Samet, J.M. and Dominici, F. (2004). Ozone and Short-term Mortality in 95 US Urban Communities, 1987-2000. *JAMA* 292: 2372–2378.

DISCOVER-AQ mission. National Aeronautics and Space Administration (NASA), http://www.nasa.gov/mission_pages/DISCOVER-AQ/index.html, Accessed 26 Feb. 2012.

Heffter, J.L. (1980). *Air resources laboratories atmospheric transport and dispersion model.* National Oceanic and Atmospheric Administration, Silver Spring, MD, USA. Air Resources Lab. NOAA-TM-ERL-ARL-81.

Johnson, B.J., Oltmans, S.J., Vömel, H., Smit, H.G.J., Deshler, T. and Kröger, C. (2002). Electrochemical concentration cell (ECC) ozonesonde pump efficiency measurements and tests on the sensitivity to ozone of buffered and unbuffered ECC sensor cathode solutions. *J. Geophys. Res.* 107: 4393.

Karl, T.R., Gleason, B.E., Menne, M.J., McMahon, J.R., Heim, R.R., Brewer, M.J., Kunkel, K.E., Arndt, D.S., Privette, J.L., Bates, J.J., Groisman, P.Y. and Easterling, D.R. (2012). U.S. temperature and drought: Recent anomalies and trends. *Eos Trans. AGU* 93: 473.

Luzik, A.M. (2009). Quantifying forest fire enhancement of the free tropospheric ozone column during the IONS-04, IONS-06, and ARC-IONS campaigns, http://etda.libraries.psu.edu/theses/approved/WorldWideIndex/ETD-3889/index.html.

Morris, G.A., Hersey, S., Thompson, A.M., Pawson, S., Nielsen, J.E., Colarco, P.R., McMillan, W.W., Stohl, A., Turquety, S., Warner, J., Johnson, B.J., Kucsera, T.L., Larko, D.E., Oltmans, S.J. and Witte, J.C. (2006). Alaskan and Canadian forest fires exacerbate ozone pollution over Houston, Texas, on 19 and 20 July 2004. *J. Geophys. Res.* 111: D24S03.

Morris, G.A., Ford, B., Rappenglück, B., Thompson, A.M., Mefferd, A., Ngan, F. and Lefer, B. (2010). An evaluation of the interaction of morning residual layer and afternoon mixed layer ozone in Houston using ozonesonde data. *Atmos. Environ.* 44: 4024–4034.

NCEP Operational Plotting Page. Physical Sciences Division, http://www.esrl.noaa.gov/psd/data/histdata/, Accessed 26 Feb. 2012.

Neu, U., Kunzle, T. and Wanner, H. (1994). On the relation between ozone storage in the residual layer and the daily variation in near surface ozone concentration case study. *Boundary Layer Meteorol.* 69: 221–247.

Payne, M.K., Joseph, E., Sakai, R., Fuentes, J.D. and Stockwell, W.R. (2015). Meteorological controls on particle growth events in Beltsville, MD, USA during July 2011. *J. Atmos. Chem.* 72: 423–440.

Pierce, R.B. and Grant, W.B. (1998). Seasonal evolution of Rossby and gravity wave induced laminae in ozonesonde data obtained from Wallops Island, Virginia. *Geophys. Res. Lett.* 43: 1859–1862.

Salmond, J.A. and McKendry I.G. (2002). Secondary ozone maxima in a very stable nocturnal boundary layer: Observations from the Lower Fraser Valley, B.C. *Atmos. Environ.* 36: 5771–5782.

Singh, H., Brune, W., Crawford, J., Jacob, D.J. and Russel, P. (2006). Overview of the summer 2004 intercontinental chemical transport experiment–North America (INTEX-A). *J. Geophys. Res.* 111: D24S01.

Stauffer, R.M., Thompson, A.M., Martins, D.K., Clark, R.D., Goldberg, D.L., Loughner, C.P., Delgado, R., Dickerson, R.R., Stehr, J.W. and Tzortziou, M.A. (2015). Bay breeze influence on surface ozone at Edgewood, MD during July 2011. *J. Atmos. Chem.* 72: 335–353.

Stohl, A., Bonasoni, P., Cristofanelli, P., Collins, W., Feichter, J., Frank, A., Forster, C., Gerasopoulos, E., Gäggeler, H., James, P., Kentarchos, T., Kromp-Kolb, H., Krüger, B., Land, C., Meloen, J., Papayannis, A., Priller, A., Seibert, P., Sprenger, M., Roelofs, G.J., Scheel, H.E., Schnabel, C., Siegmund, P., Tobler, L., Trickl, T., Wernli, H., Wirth, V., Zanis, P. and Zerefos, C. (2003). Stratosphere-troposphere exchange: A review and what we have learned from STACCATO. *J. Geophys. Res.* 108: 8516

Teitelbaum, H., Ovarlez, J., Kelder, H. and Lott, F. (1994). Some observations of gravity-wave-induced structure in ozone and water vapour during EASOE. *Geophys. Res. Lett.* 21: 1483–1486.

Teitelbaum, H. (1996). The role of atmospheric waves in the laminated structure of ozone profiles at high latitude. *Tellus* 49: 442–455.

Thompson, A.M., Doddridge, B.G., Witte, J.C., Hudson, R.D., Luke, W.T., Johnson, J.E., Johnson, B.J., Oltmans, S.J. and Weller, R. (2000). A tropical Atlantic paradox: Shipboard and satellite views of a tropospheric ozone maximum and wave-one in January–February 1999. *Geophys. Res. Lett.* 27: 3317–3320.

Thompson, A.M., Stone, J.B., Witte, J.C., Miller, S.K., Pierce, R.B., Chatfield, R.B., Oltmans, S.J., Cooper, O.R., Loucks, A.L., Taubman, B.F., Johnson, B.J., Joseph, E., Kucsera, T.L., Merrill, J.T., Morris, G.A., Hersey, S., Forbes, G., Newchurch, M.J., Schmidlin, F.J., Tarasick, D.W., Thouret, V. and Cammas, J.P. (2007a). Intercontinental Chemical Transport Experiment Ozonesonde Network Study (IONS) 2004: 1. Summertime upper troposphere/lower stratosphere ozone over northeastern North America. *J. Geophys. Res.* 112: D12S12.

Thompson, A.M., Stone, J.B., Witte, J.C., Miller, S.K., Oltmans, S.J., Kucsera, T.L., Ross, K.L., Pickering, K.E., Merrill, J.T., Forbes, G., Tarasick, D.W., Joseph, E., Schmidlin, F.J., McMillan, W.W., Warner, J., Hintsa, E.J. and Johnson, J.E. (2007b). Intercontinental Chemical Transport Experiment Ozonesonde Network Study (IONS) 2004: 2. Tropospheric ozone budgets and variability over northeastern North America. *J. Geophys. Res.* 112: D12S13.

Thompson, A.M., Witte, J.C., Smit, H.G.J., Oltmans, S.J., Johnson, B.J., Kirchhoff, V.W.J.H. and Schmidlin, F.J. (2007c). Southern Hemisphere Additional Ozonesondes (SHADOZ) 1998-2004 tropical ozone climatology: 3. Instrumentation, station-to-station variability, and evaluation with simulated flight profiles. *J. Geophys. Res.* 112: D03304.

Thompson, A.M., Miller, S.K., Tilmes, S., Kollonige, D.W., Witte, J.C., Oltmans, S.J., Johnson, B.J., Fujiwara, M., Schmidlin, F.J., Coetzee, G.J.R., Komala, N., Maata, M., Mohamad, M.b., Nguyo, J., Mutai, C., Ogino, S.Y., Silva, F.R.D., Leme, N.M.P., Posny, F., Scheele, R., Selkirk, H.B., Shiotani, M., Stübi, R., Levrat, G., Calpini, B., Thouret, V., Tsuruta, H., Canossa, J.V., Vömel, H., Yonemura, S., Diaz, J.A., Thanh, N.T.T. and Ha, H.T.T. (2012). Southern Hemisphere Additional Ozonesondes (SHADOZ) ozone climatology (2005-2009): Tropospheric and tropical tropopause layer (TTL) profiles with comparisons to OMI-based ozone products. *J. Geophys. Res.* 117: D23301.

Thompson, A.M., Stauffer, R.M., Miller, S.K., Martins, D.K., Joseph, E., Weinheimer, A.J. and Diskin, G.S. (2015). Ozone profiles in the Baltimore-Washington Region (2006-2011): Satellite comparisons and DISCOVER-AQ observations. *J. Atmos. Chem.* 72: 393–422.

Tong, N.Y.O., Leung, D.Y.C. and Liu, C.H. (2011). A review on ozone evolution and its relationship with boundary layer characteristics in urban environments. *Water Air Soil Pollut.* 214: 13–36.

Yorks, J.E., Thompson, A.M., Joseph, E. and Miller, S.K. (2009). The variability of free tropospheric ozone over Beltsville, Maryland (39N, 77W) in the summers 2004-200. *Atmos. Environ.* 43: 1827–1838.

Zhang, J. and Rao, S.T. (1999). The role of vertical mixing in the temporal evolution of ground-level ozone concentrations. *J. Appl. Meteorol. Climatol.* 38: 1674–1691.

Received for review, December 12, 2017
Revised, March 16, 2018
Accepted, March 26, 2018